

## Probing the ATP Ribose-Binding Domain of Cyclin-Dependent Kinases 1 and 2 with *O*<sup>6</sup>-Substituted Guanine Derivatives

Ashleigh E. Gibson,<sup>†</sup> Christine E. Arris,<sup>‡</sup> Johanne Bentley,<sup>‡</sup> F. Thomas Boyle,<sup>§</sup> Nicola J. Curtin,<sup>‡</sup> Thomas G. Davies,<sup>||</sup> Jane A. Endicott,<sup>||</sup> Bernard T. Golding,<sup>†</sup> Sharon Grant,<sup>†</sup> Roger J. Griffin,<sup>†</sup> Philip Jewsbury,<sup>§</sup> Louise N. Johnson,<sup>||</sup> Veronique Mesguiche,<sup>†</sup> David R. Newell,<sup>\*,‡</sup> Martin E. M. Noble,<sup>||</sup> Julie A. Tucker,<sup>||</sup> and Hayley J. Whitfield<sup>†,‡</sup>

Department of Chemistry and Cancer Research Unit, University of Newcastle, Newcastle upon Tyne, NE2 4HH, United Kingdom, AstraZeneca Pharmaceuticals, Alderley Park, Cheshire, SK10 4TG, United Kingdom, and Laboratory of Molecular Biophysics, Department of Biochemistry, University of Oxford, Oxford, OX1 3QU, United Kingdom

Received February 6, 2002

*O*<sup>6</sup>-Substituted guanines are adenosine 5'-triphosphate (ATP) competitive inhibitors of CDK1/cyclin B1 and CDK2/cyclin A, the *O*<sup>6</sup> substituent occupying the kinase ribose binding site. Fifty-eight *O*<sup>6</sup>-substituted guanines were prepared to probe the ribose pocket, and the structures of four representative compounds bound to monomeric CDK2 were determined by X-ray crystallography. Optimum binding occurs with a moderately sized aliphatic *O*<sup>6</sup> substituent that packs tightly against the hydrophobic patch presented by the glycine loop, centered on Val18, an interaction promoted by the conformational restraints imposed in a cyclohexylmethyl or cyclohexenylmethyl ring. Structure-based design generated (*R*)-(2-amino-9*H*-purin-6-ylloxymethyl)pyrrolidin-2-one (**56**), which reproduces the reported hydrogen bonds formed between ATP and Asp86 and Gln131 but failed to improve inhibitory potency. Thus, the parent compound *O*<sup>6</sup>-cyclohexylmethylguanine (NU2058, **25**) is the preferred starting point for exploring other areas of the kinase active site.

### Introduction

Cyclin-dependent kinases (CDKs) are attracting considerable attention as targets for therapeutic intervention in cancer as well as nonneoplastic proliferative diseases, and first generation compounds are in clinical trials.<sup>1,2</sup> A large number of CDK inhibitory pharmacophores have been identified, and the majority of the nonpeptide inhibitors interacts with CDKs at the adenosine 5'-triphosphate (ATP) binding site.<sup>3–5</sup> Recently, we identified two novel substituted guanine and pyrimidine CDK inhibitory pharmacophores, which were shown to be inhibitors of CDK1/cyclin B1 and CDK2/cyclin A.<sup>6</sup> The compounds bind to monomeric CDK2 in an orientation distinct from that of the majority of the purine-based inhibitors such as olomoucine, roscovitine, and purvalanol.<sup>7–9</sup> The lead guanine-based inhibitor, *O*<sup>6</sup>-cyclohexylmethylguanine (NU2058, **25**), is a competitive inhibitor of CDK1 and CDK2 with respect to ATP (*K*<sub>i</sub> values = CDK1, 5 ± 1 μM; CDK2, 12 ± 3 μM). NU2058 forms a triplet of hydrogen bonds within the CDK2 ATP binding site, i.e., NH-9 to the backbone carbonyl group of Glu 81 and N-3 and 2-NH<sub>2</sub> to the backbone carbonyl and amide groups, respectively, of Leu 83. The *O*<sup>6</sup>-cyclohexylmethyl group of NU2058 occupies the ribose binding pocket of CDK2. NU2058 inhibits the growth of human tumor cells (mean GI<sub>50</sub> value 13 ± 7 μM in the National Cancer Institute,

U.S.A., cell line panel), with a pattern of activity distinct from that of flavopiridol and olomoucine.<sup>6</sup>

The current paper describes studies to define structure–activity relationships (SAR) for *O*<sup>6</sup>-substituted guanine derivatives. These studies were performed in an attempt to improve the potency and selectivity of CDK1 and CDK2 inhibition by exploring the ribose binding pocket of the enzymes. Selected compounds were soaked into monomeric CDK2 crystals, to define further inhibitor–enzyme interactions and to guide inhibitor design. In addition, representative compounds were tested for their ability to inhibit human tumor cell growth in vitro.

### Chemistry

With the exception of the compounds listed in the Experimental Section, inhibitors were prepared as previously described.<sup>6,10,11</sup> The preparation of *O*<sup>6</sup>-substituted purines has been well-documented in the literature. Previous syntheses of compounds derived from simple alcohols utilized commercially available 2-amino-6-chloropurine as starting material, with the alcohol as solvent or employing a cosolvent.<sup>10,12</sup> However, with less reactive alcohols, activation of the 6-position is required to achieve a satisfactory rate of displacement. Thus, a number of activated purine derivatives have been employed to enhance reactivity at this position, including 2-amino-6-trimethylammonium purine.<sup>13,14</sup> We have previously reported the use of 2-amino-6-(1-azonia-4-azabicyclo[2.2.2]oct-1-yl)purine chloride (DABCO-purine) as a convenient and readily prepared reagent for the introduction of 6-alkoxy substituents.<sup>11,15</sup> This quaternary ammonium salt also offers the advantage of being readily separable from the

\* To whom correspondence should be addressed. Tel: -44-191-222-8057. Fax: -44-191-222-7556. E-mail: herbie.newell@ncl.ac.uk.

<sup>†</sup> Department of Chemistry, Newcastle University.

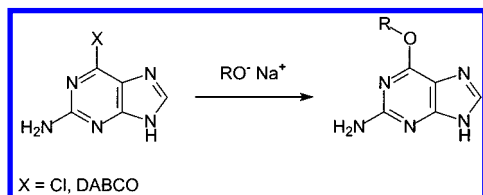
<sup>‡</sup> Cancer Research Unit, Newcastle University.

<sup>§</sup> AstraZeneca Pharmaceuticals.

<sup>||</sup> University of Oxford.

<sup>‡</sup> This paper is dedicated to the memory of Hayley J. Whitfield.

Scheme 1

Table 1. Inhibition of CDKs 1 and 2 by *O*<sup>6</sup>-Alkylguanines

compd	R	CDK inhibition (IC <sub>50</sub> (μM) or % inhibition at the concentration indicated)	
		CDK1/cyclin B	CDK2/cyclin A
1	Me	36 ± 1% (100 μM)	35 ± 1% (100 μM)
2	Et	48 ± 1% (100 μM)	51 ± 5% (100 μM)
3	<i>n</i> -Pr	75 ± 7	67 ± 5
4	<i>n</i> -Bu	32 ± 3	48 ± 7
5	Me(CH <sub>2</sub> ) <sub>3</sub> CH <sub>2</sub>	37 ± 6	49 ± 7
6	Me(CH <sub>2</sub> ) <sub>5</sub> CH <sub>2</sub>	62 ± 6	>100 μM
7	<i>i</i> -Pr	75 ± 14	75 ± 10
8	EtCH(Me)	27 ± 3	25 ± 1
9	(Me) <sub>2</sub> CHCH <sub>2</sub>	45 ± 8	42 ± 5
10	EtCH(Me)CH <sub>2</sub>	17 ± 1	15 ± 2
11	(Me) <sub>2</sub> CHCH <sub>2</sub> CH <sub>2</sub>	21 ± 4	26 ± 9

*O*<sup>6</sup>-alkylpurine, thereby aiding product purification. In this study, the choice of purine starting material varied according to the alkoxide employed, which was readily generated by reaction of the appropriate alcohol with sodium or sodium hydride (see standard procedures A–C, Scheme 1).

## Results and Discussion

**SAR for CDK1 and CDK2 Inhibition.** Initial studies explored the inhibition of CDK1/cyclin B1 and CDK2/cyclin A by simple *O*<sup>6</sup>-alkylguanines. Homologation from *O*<sup>6</sup>-methylguanine (**1**) to *O*<sup>6</sup>-butylguanine (**4**) and *O*<sup>6</sup>-pentylguanine (**5**) resulted in an increase in both CDK1 and CDK2 inhibition with greater chain length. However, there was no differential inhibition of the two CDKs and extension beyond **5** resulted in reduced potency (Table 1). The introduction of branched alkyl chains either had no effect on activity (**7** and **9**) or resulted in increased activity (**8** – CDK2; **10** and **11** – CDK1 and 2), relative to the corresponding linear alkyl derivative (Table 1). Notably, compound **10**, which may be regarded as most closely resembling NU2058 (**25**), showed maximal activity among the linear or branched chain alkyl derivatives investigated and was equipotent with **25** against CDK2. However, **10** proved 2–3-fold less potent than **25** against CDK1. Overall, the activity of the *O*<sup>6</sup>-alkylguanines is consistent with the presence of a hydrophobic pocket in the ribose binding domain, which can accommodate lipophilic groups of appropriate size (see below). Furthermore, *O*<sup>6</sup>-alkyl substituent binding at this site influences potency but not CDK specificity.

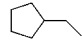
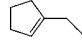
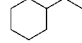


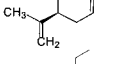
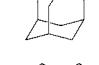
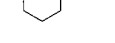
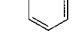
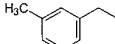
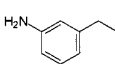
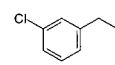
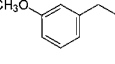
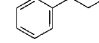
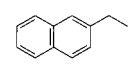
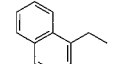
Table 2. Inhibition of CDKs 1 and 2 by *O*<sup>6</sup>-Alkenyl-, *O*<sup>6</sup>-Alkenyl-, and *O*<sup>6</sup>-(2-Oxo)alkylguanines

Compd.	R	CDK inhibition (IC <sub>50</sub> (μM) or % inhibition at the concentration indicated)	
		CDK1/Cyclin B	CDK2/Cyclin A
12	CH=CCH <sub>2</sub>	91 ± 6	90 ± 7
13	CH <sub>2</sub> =CH(CH <sub>2</sub> ) <sub>3</sub> CH <sub>2</sub>	41 ± 4	47 ± 4
14	<i>E</i> -EtCH=CHCH <sub>2</sub> CH <sub>2</sub>	76 ± 6	69 ± 8
15	CH <sub>2</sub> =CHCH <sub>2</sub>	68 ± 10	78 ± 13
16	CH <sub>2</sub> =C(Me)CH <sub>2</sub>	32 ± 9	35 ± 6
17	CH <sub>2</sub> =C(Et)CH <sub>2</sub>	19 ± 2	21 ± 2
18	CH <sub>2</sub> =C( <i>i</i> -Pr)CH <sub>2</sub>	11 ± 1	16 ± 1
19		25 ± 1	34 ± 3
20		21 ± 4% (10 μM)	12 ± 4% (10 μM)
21	MeC(O)CH <sub>2</sub>	15 ± 3% (100 μM)	16 ± 3% (100 μM)
22	<i>i</i> -PrC(O)CH <sub>2</sub>	41 ± 8% (100 μM)	31 ± 3% (100 μM)

The introduction of unsaturation into the *O*<sup>6</sup>-alkyl substituent was tolerated, with *O*<sup>6</sup>-propargyl- (**12**) and *O*<sup>6</sup>-allylguanines (**15**) (Table 2) exhibiting activity comparable with the *O*<sup>6</sup>-propyl derivative (**3**) (Table 1), while the alkene **17** was of similar potency to the corresponding saturated derivative (**10**). The most potent *O*<sup>6</sup>-alkenylguanine was the *O*<sup>6</sup>-isopropallylguanine (**18**), which had IC<sub>50</sub> values for both CDK1 and CDK2 inhibition similar to those of NU2058 (**25**). Consistent with there being a ribose pocket that can accept considerable steric bulk, the phenylallyl derivative **19** retained much of the activity of compounds **16**–**18**. Unfortunately, the poor solubility of the cyclohexylidene analogue **20** precluded studies with this compound at concentrations greater than 10 μM, where only weak CDK inhibition (<25%) was observed. Of interest is the observation that the 6-(2'-oxoalkyl)purine analogues **21** and **22** were both markedly less active than their corresponding isosteric alkenyl derivatives **16** and **18**, suggesting that their carbonyl substituents are unable to form sufficiently favorable hydrogen bonds within the ribose binding domain.

In light of the interesting activity exhibited by the *O*<sup>6</sup>-cyclohexylmethylpurine **25**, a number of analogous *O*<sup>6</sup>-cycloalkylmethyl- and *O*<sup>6</sup>-cycloalkenylmethyl derivatives were synthesized and evaluated. *O*<sup>6</sup>-Cyclopentylmethylguanine **23** was less active than **25** against CDK1 but of similar potency as an inhibitor of CDK2 (Table 3). The introduction of a double bond at the 1-position of the *O*<sup>6</sup>-cyclopentylmethyl and *O*<sup>6</sup>-cyclohexylmethyl derivatives to afford **24** and **26**, respectively, reduced potency as compared with the parent cycloalkylmethylguanines **23** and **25**. In contrast, the *O*<sup>6</sup>-cyclohex-3-

**Table 3.** Inhibition of CDKs 1 and 2 by *O*<sup>6</sup>-(Cycloalkyl)methyl- and *O*<sup>6</sup>-Benzylguanines

Compd.	R	CDK inhibition (IC <sub>50</sub> (μM) or % inhibition at the concentration indicated)	
		CDK1/Cyclin B	
		CDK1/Cyclin B	CDK2/Cyclin A
23		15 ± 1	21 ± 4
24		19 ± 8	31 ± 7
25		7 ± 1	17 ± 2
26		11 ± 3	22 ± 4
27		6 ± 1	13, 19
28		17 ± 7% (10 μM)	18 ± 15% (10 μM)
29		55 ± 1% (10 μM)	29 ± 10% (10 μM)
30		37 ± 6	44 ± 3
31		24 ± 3	35 ± 6
32		70 ± 1% (100 μM)	52 ± 7% (100 μM)
33		65 ± 1% (100 μM)	52 ± 3% (100 μM)
34		28 ± 4% (10 μM)	19 ± 1% (10 μM)
35		65 ± 1% (100 μM)	49 ± 14% (10 μM)
36		59 ± 7	65 ± 6
37		12 ± 4% (10 μM)	9 ± 8% (10 μM)
38		10 ± 4% (10 μM)	3 ± 4% (10 μM)

enylmethyl derivative (**27**) had similar activity to **25** against both enzymes. Replacement of the cyclohexyl group of **25** with a phenyl group to give *O*<sup>6</sup>-benzyl-guanine (**31**) resulted in a 2–3-fold reduction in activity against both kinases, whereas substitution on the *O*<sup>6</sup>-benzyl group (**32**, **33**, and **35**) resulted in a marked loss of potency. The effect of chloro substitution could not be fully defined, because of the poor solubility of **34**.

Homologation of **25** and **31** to give *O*<sup>6</sup>-cyclohexylethyl-guanine (**30**) and *O*<sup>6</sup>-phenylethyl-guanine (**36**), respectively, reduced inhibitory activity against both enzymes, an observation that is consistent with a ribose binding

**Table 4.** Inhibition of CDKs 1 and 2 by *O*<sup>6</sup>-Hydroxyalkyl- and *O*<sup>6</sup>-Alkoxyalkylguanines

compd	R	CDK inhibition (IC <sub>50</sub> (μM) or % inhibition at the concentration indicated)	
		CDK1/cyclin B	
		CDK1/cyclin B	CDK2/cyclin A
39	HOCH <sub>2</sub> CH(OH)CH <sub>2</sub>	35 ± 8% (100 μM)	33 ± 12% (100 μM)
40	MeOCH <sub>2</sub> –CH(OMe)CH <sub>2</sub>	49 ± 9% (100 μM)	41 ± 5% (100 μM)
41	MeC(OEt) <sub>2</sub> CH <sub>2</sub>	36 ± 8	33 ± 6
42	EtC(OMe) <sub>2</sub> CH <sub>2</sub>	19 ± 2	20 ± 5

pocket of limited dimensions. Attempts to probe the ribose-binding domain with bulky cycloalkyl (**28** and **29**) or aromatic groups (**37** and **38**) were compromised by the poor solubility of these compounds in the CDK assay buffers. However, with the exception of *O*<sup>6</sup>-adamantyl-methyl-guanine (**29**), which had activity comparable to **25**, CDK inhibition at 10 μM was relatively weak (<25%).

With a view to exploiting known H-bonding interactions within the ribose binding pocket of CDK2,<sup>7</sup> a number of guanine derivatives bearing *O*<sup>6</sup>-hydroxyalkyl and *O*<sup>6</sup>-alkoxyalkyl functions (**39**–**42**) were investigated (Table 4). None of the compounds was as active as **25**, although in comparison to the corresponding linear *O*<sup>6</sup>-alkyl derivatives (**3** and **4**) the 2',2'-dialkoxy compounds **41** and **42** were approximately 2-fold more active and similar in activity to the branched chain *O*<sup>6</sup>-alkyl-guanines (**9**–**11**) and *O*<sup>6</sup>-alkenylguanines (**16**–**18**). In contrast, the *O*<sup>6</sup>-(2',3'-dihydroxypropyl)- and *O*<sup>6</sup>-(2',3'-dimethoxypropyl)guanines (**39** and **40**) were less active than *O*<sup>6</sup>-propyl-guanine (**3**).

As an alternative approach to exploiting potential H-bonding interactions in the ribose binding pocket, a series of guanine derivatives bearing heterocyclic (**43**–**56**) or pyridyl groups (**57** and **58**) at the *O*<sup>6</sup>-position were evaluated (Table 5). Where comparisons could be made, these derivatives were markedly less active than the corresponding *O*<sup>6</sup>-cycloalkylmethyl or *O*<sup>6</sup>-benzyl derivatives, and in general, no pronounced inhibition of either CDK1 or CDK2 was observed. Hence, the derivatives investigated were either unable to exploit potential H-bonding interactions in the ribose binding pocket, or such interactions do not confer increased potency for CDK inhibition. Structural studies were performed with selected compounds (see below) to address these two possibilities.

The above structure–activity studies demonstrate that a broad range of substituents are tolerated at the *O*<sup>6</sup>-position but that none result in improved activity or specificity of CDK1 vs CDK2 inhibition over that seen with the lead compound NU2058 (**25**). On the contrary, certain modifications appear to be deleterious, notably: substitution with oxygen at the 2'-position of the alkyl chain, introduction of heterocyclic or pyridyl derivatives, and nonoptimal size for lipophilic groups.

For CDK inhibitors based on the 6-aminopurine pharmacophore, as exemplified by olomoucine, rosco-

**Table 5.** Inhibition of CDKs 1 and 2 by *O*<sup>6</sup>-Heterocyclomethylguanines

Compd.	R	CDK inhibition (IC <sub>50</sub> (μM) or % inhibition at the concentration indicated)	
		CDK1/Cyclin B	
		CDK1/Cyclin B	CDK2/Cyclin A3
43		49 ± 7% (100 μM)	40 ± 3% (100 μM)
44		10 ± 3% (100 μM)	16 ± 5% (100 μM)
45		43 ± 8% (100 μM)	36 ± 5% (100 μM)
46		46 ± 4% (100 μM)	39 ± 2% (100 μM)
47		31 ± 3% (100 μM)	27 ± 3% (100 μM)
48		39 ± 12	65 ± 2
49		26 ± 7% (100 μM)	29 ± 3% (100 μM)
50		50 ± 4% (100 μM)	43 ± 2% (100 μM)
51		10 ± 6% (100 μM)	4 ± 5% (100 μM)
52		52 ± 2% (100 μM)	52 ± 2% (100 μM)
53		70 ± 1% (100 μM)	64 ± 6% (100 μM)
54		52 ± 2% (100 μM)	43 ± 7% (100 μM)
55		22 ± 6% (100 μM)	15 ± 5% (100 μM)
56		50 ± 5% (100 μM)	35 ± 4% (100 μM)
57		58 ± 8% (100 μM)	43 ± 5% (100 μM)
58		55 ± 3% (100 μM)	43 ± 3% (100 μM)

vitine, and purvalanol, the substituent at the 2-position of the purine ring occupies the ribose binding pocket of CDK2.<sup>7–9</sup> Consistent with the data in the current investigation, SAR studies for inhibition of CDK1 and/or CDK2 by 2-substituted 6-aminopurines have shown that an extremely diverse range of groups is tolerated,<sup>8,9,16–21</sup> assuming that the derivatives bind to the enzymes in the same orientation to that of olomoucine,

roscovitine, and purvalanol, which for at least one such compound (OL567) has been shown to be the case.<sup>21</sup> These 2-substituents include straight chain and branched alkylamino, alkyl, alkenyl, and alkynyl groups, as well as cyclic amines, many with hydroxyl substituents. Together with the results in the current study, the data for 6-aminopurine CDK inhibitors suggest that the ribose pocket, provided it is adequately occupied but not overfilled, does not contribute greatly to the potency or selectivity of CDK inhibition.

**Structural Studies of the Binding of Representative *O*<sup>6</sup>-Substituted Guanines to Monomeric CDK2.** To rationalize the SAR observed for the *O*<sup>6</sup>-substituted guanines (Tables 1–5), the structures of four inhibitors complexed with monomeric CDK2 were determined using X-ray crystallography. The inhibitors studied were chosen with the aim of examining protein–ligand interactions formed by a representative range of *O*<sup>6</sup> substituents including unsaturated **27**, acyclic **22**, and polar (**43** and **56**) groups, and the results were compared to the previously described structure of the purely hydrophobic cyclohexylmethyl derivative **25**.<sup>6</sup>

Monomeric unphosphorylated CDK2 represents the minimal catalytic kinase core and consists of a smaller (approximately 80 residues) N-terminal domain composed predominantly of  $\beta$ -strands and a larger (210 residues) C-terminal domain, which is mainly  $\alpha$ -helical.<sup>7,22</sup> These two domains are linked by a short hinge region (residues 81–84), and the ATP binding site is located in a deep cleft between them (Figure 1a). In all cases, the overall fold of CDK2 was unperturbed by inhibitor binding and a superposition revealed no major structural changes (Figure 1b). However, the quality of the electron density map was very variable for residues in the activation loop (containing the Thr160 phosphorylation site) and in some structures was of insufficient quality to build all residues with confidence.

The binding mode of the *O*<sup>6</sup>-alkylguanine-based inhibitors to CDK2 has been previously elucidated by X-ray crystallography.<sup>6</sup> Studies on the monomeric CDK2–NU2058 complex presented previously revealed that the purine ring binds in the ATP binding cleft, forming a triplet of hydrogen bonds between residues in the hinge region of CDK2 and the N2, N3, and N9 atoms of the inhibitor.<sup>6</sup> The purine ring system is sandwiched between the N- and the C-terminal domains of the kinase with which it forms a number of hydrophobic contacts. Both the triplet of hydrogen bonds and the purine–CDK2 packing interactions are conserved in all five CDK2–inhibitor structures described here and are shown in schematic form in Figure 2a. The purine core occupies a similar region of the pocket in all structures although some minor variations occur, presumably to accommodate differences in the shape of the *O*<sup>6</sup> substituent (Figure 2b,c). Although the *O*<sup>6</sup>-cyclohexyl substituent of NU2058 (**25**) binds in a position close to that occupied by the ribose group of ATP, the interactions of the *O*<sup>6</sup> substituent are predominantly hydrophobic, with highly complementary packing arising between the cyclohexane ring and an apolar patch on the glycine loop contributed predominantly by the side chain of Val18 (Figure 3).

As described above (Table 3), the effect on CDK inhibition of introducing unsaturation into the cyclo-



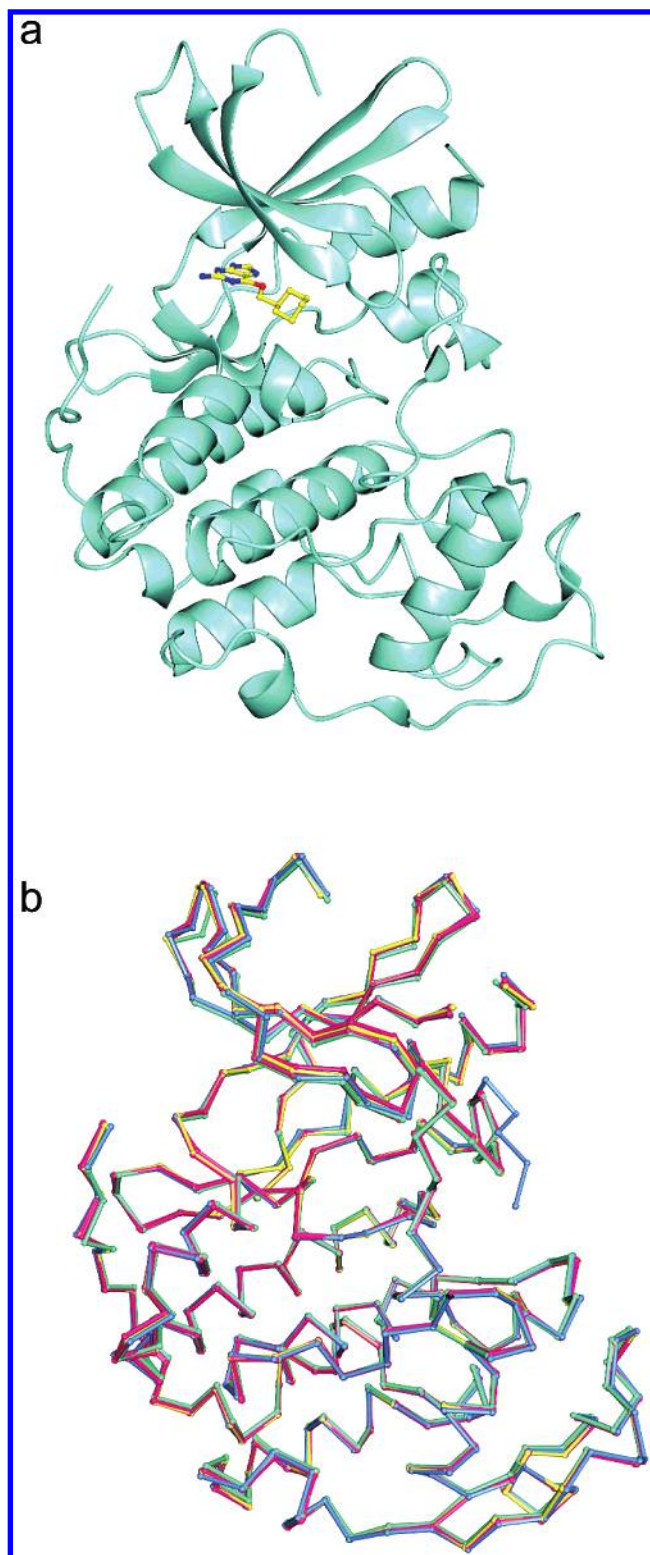


**Figure 1.** (a) Overall structure of monomeric CDK2–NU2058 (**25**) complex. The CDK2 fold is rendered in ribbon representation and colored green. The inhibitor NU2058 is drawn in ball-and-stick mode with carbon, nitrogen, and oxygen atoms colored yellow, blue, and red, respectively. (b) Overlay of CDK2 C $\alpha$  atoms of the five CDK2–inhibitor complexes. The C $\alpha$  traces for CDK2 bound to each inhibitor are colored red (for CDK2 bound to inhibitor **22**), mint (bound to **25**), yellow (bound to **43**), white (bound to **56**), and blue (bound to **27**).

hexane ring of NU2058 is dependent upon the position of the double bond within the ring. Introduction of a double bond at the 1,2-position (as exemplified by **26**)

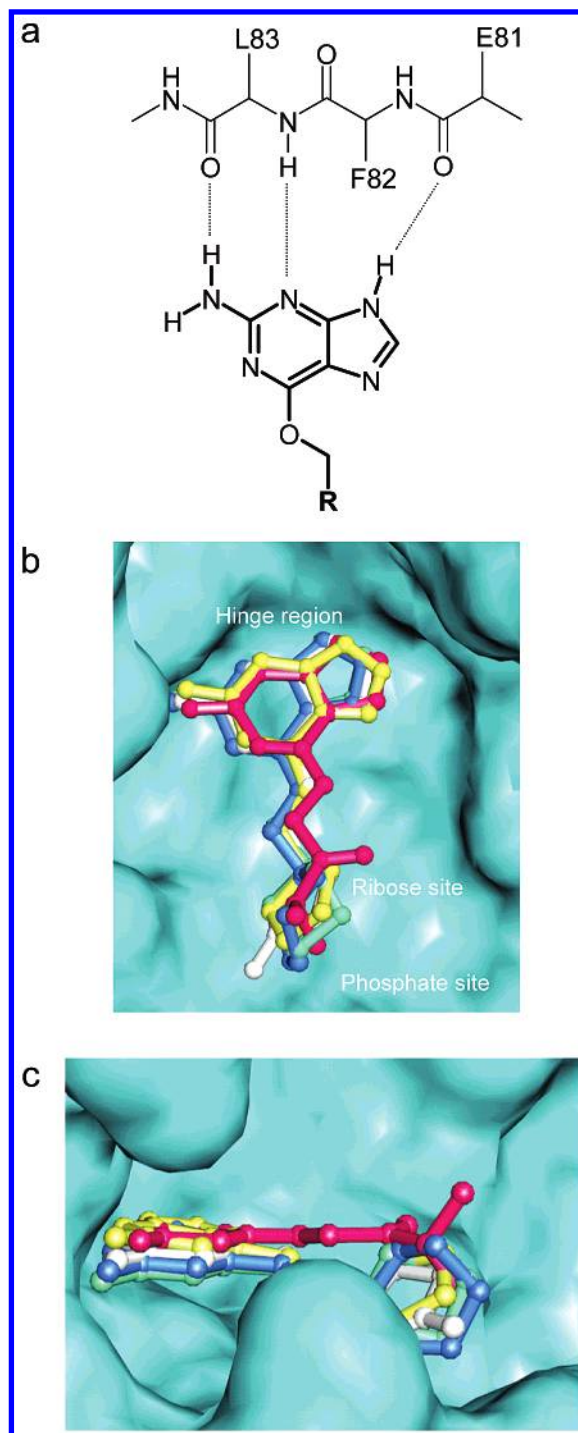


**Figure 2.** (a) Schematic representation of hydrogen bonds formed by  $O^6$ -substituted purines and the CDK2 hinge region. (b) Overlay of five inhibitors in the ATP binding site of CDK2 to illustrate main subsites. The inhibitors are drawn in ball-and-stick mode and colored as follows: **22** (red), **25** (mint), **43** (yellow), **56** (white), and **27** (blue). The solvent accessible surface of CDK2 is shown in turquoise. (c) Edge-on view of inhibitors, overlaid and colored as in b.

reduced inhibitory activity, while compound **27** (which contains a double bond at the 2,3-position) retained the activity of the parent compound. These differences may be explained by subtle alterations to protein–ligand packing as a result of changes in the shape of the  $O^6$  moiety due to differential flattening and ring pucker between compounds. The structure of **27** bound to CDK2 shows that the cyclohexene ring occupies a very similar

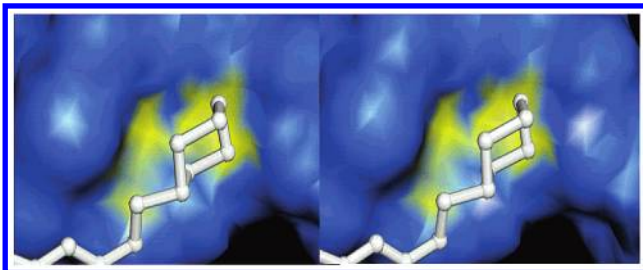


**Figure 3.** CDK2–inhibitor interactions in the ribose binding pocket. The solvent accessible surface of part of the glycine-rich loop of CDK2 is colored by hydrophobicity as calculated using GRID.<sup>39</sup> Yellow areas indicate hydrophobic regions, and blue areas indicate nonhydrophobic surfaces. The cyclohexane ring of NU2058 (**25**), drawn in white in ball-and-stick representation, is seen to pack with a hydrophobic pocket on CDK2.

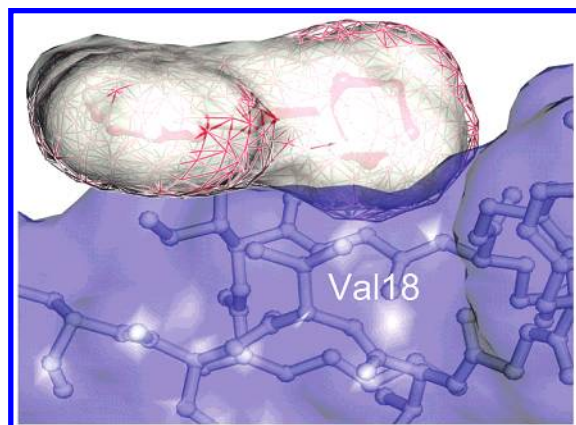


**Figure 4.** The  $O^6$  substituent of compound **27** and NU2058 (**25**) is similar in shape. The solvent accessible surface area for compound **27** is rendered as a red net and that of NU2058 (**25**) is rendered as a solid white surface. Packing of the  $O^6$  substituent with the hydrophobic pocket on the glycine-rich loop (colored as a blue surface) is present in each case.

position within the ribose site as the cyclohexyl group of NU2058 (**25**). An overlay of **27** and **25**, together with their associated solvent accessible surfaces, shows that they pack almost identically with the hydrophobic pocket on the glycine-rich loop (Figure 4). The electron density does not clearly identify the ring conformation, and it is probable that both enantiomers of **27** are bound. Nevertheless, when **27** is built as the dominant (*S*) enantiomer and refined with ideal geometry, the C2' carbon (which is responsible for the majority of the contacts with the glycine loop) is found in the same position as that in **25**. In contrast, introduction of a double bond at the C1'-position of the ring is predicted to lead to a flattening of the ring at this point, which would decrease the packing complementarity between CDK2 and the inhibitor.

Compound **56** was designed to mimic the hydrogen-bonding interactions of the ribose hydroxyl groups of ATP. However, enzyme inhibition data (Table 5) revealed a marked reduction in activity relative to **25**. The structure of **56** bound to monomeric CDK2 provides a rationale for this observation (Figure 5). Compound **56** is observed to bind to CDK2 in the designed mode, forming a hydrogen bond between the amide nitrogen on the  $O^6$  substituent and the Asp86 ( $r_{\text{NH-O}} = 3.1 \text{ \AA}$ ). In addition, a rather long hydrogen bond is formed between the ligand amide oxygen and the side-chain of Gln131 ( $r_{\text{O-NH}} = 3.3 \text{ \AA}$ ). Gln131 was poorly defined in

the electron density and appears to be present in two conformations, consistent with a relatively weak or energetically neutral hydrogen bond being formed with the inhibitor. Although Asp86 is considerably better positioned to accept a hydrogen bond from the inhibitor as compared to Gln131, in both cases, the geometry of interaction is suboptimal. Desolvation and removal of both inhibitor and unliganded CDK2 from bulk solvent, where hydrogen-bonding geometry will be near-optimal, is therefore likely to be enthalpically unfavorable. In the absence of protein hydrogen bond acceptors and donors with suitable geometry, the net effect on ligand binding will be a decrease in binding affinity and hence a reduction in enzyme inhibition, as observed here. Although desolvation of polar atoms on the  $O^6$  substituent provides the main explanation for the reduced inhibitory activity of **56**, the compound additionally lacks the hydrophobicity and shape complementarities to the glycine loop that are present in NU2058 (**25**). As a final caveat, it should be noted that any hydrogen bonds formed between inhibitors and monomeric CDK2 may not be present when bound to the fully active phosphoCDK2/cyclin A complex. The ribose binding site of CDK2 undergoes considerable rearrangement on activation, and a comparison of the structures of monomeric CDK2/ATP and phosphoCDK2/cyclin A/ATP shows that the protein–ribose hydrogen bonds are different in the inactive and active forms of the enzyme.<sup>22,23</sup>

The structure of **22** bound to CDK2 reveals that the  $O^6$  group of this inhibitor binds in a slightly different position to the cyclohexane ring of NU2058 (**25**). The hydrophobic isopropyl group of the  $O^6$  substituent is orientated toward the glycine loop, but its position is such that it cannot mimic the C2'-position of cyclohexane and is not complementary in shape to the hydrophobic patch formed by Val18. Instead, it forms an unfavorable apolar–polar contact with the backbone amide nitrogen of Glu12 ( $r_{\text{C-N}} = 3.1 \text{ \AA}$ ) and causes the glycine loop to shift by approximately 1  $\text{\AA}$  leading to a slight widening of the binding cleft. The carbonyl oxygen mimics the  $\alpha$ -ether oxygen of ATP and forms a long hydrogen bond with Lys33 ( $r_{\text{O-N}} = 3.6 \text{ \AA}$ ) (Figure 6). However, as for **56**, the nonideal geometry of this interaction will lead to inadequate energetic compensation for the penalty of desolvating this oxygen and Lys33. Consistent with the reduced activity of **22** (Table 2), the  $O^6$  substituent of this compound is (in both shape and chemical character) less complementary to its environment than the cyclohexylmethyl group of NU2058 (**25**).

The structure of **43** bound to CDK2 revealed that although chemically distinct, the tetrahydrofuran (THF) ring of **43** overlays with the cyclohexane ring of NU2058 (**25**). CDK2 exclusively bound the (*S*) enantiomer from the racemic **43**. The furan oxygen lies in the same position as the C2' carbon of NU2058 (**25**) and is orientated toward the hydrophobic pocket formed by Val18 on the glycine loop (Figure 7). To satisfy the hydrogen-bonding potential of Lys 33 and the furan oxygen, a water molecule forms a bridge between the Lys33 and the inhibitor through two hydrogen bonds ( $r_{\text{O-O}} = 2.2 \text{ \AA}$ ) and Lys33 ( $r_{\text{O-N}} = 2.9 \text{ \AA}$ ). However, the sequestration of the water molecule is likely to carry



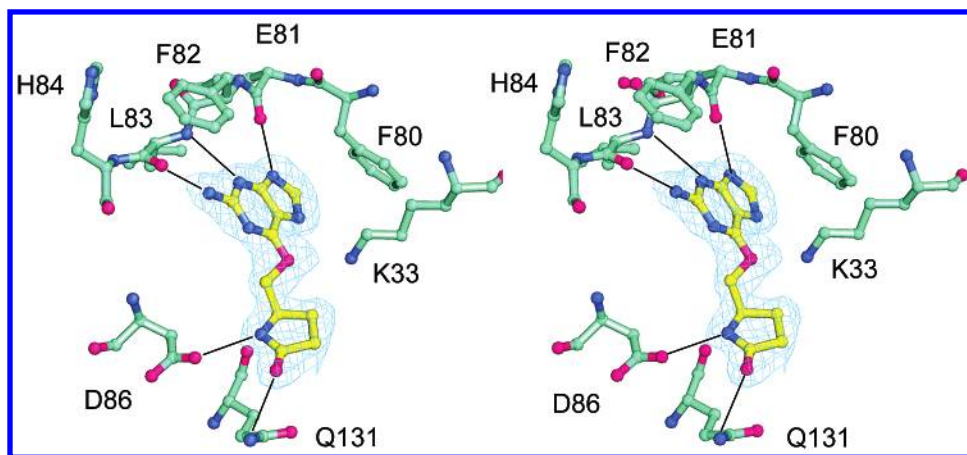


**Figure 5.** Stereoview of compound **56** bound to CDK2. Selected protein residues are drawn in ball-and-stick mode with carbon atoms colored green, nitrogen atoms colored blue, and oxygen atoms colored red. Hydrogen bonds are denoted by dashed lines. Only one conformation of Gln131 is represented. The final  $2F_o - F_c$  electron density map is shown for the ligand (contoured at  $1\sigma$ ).

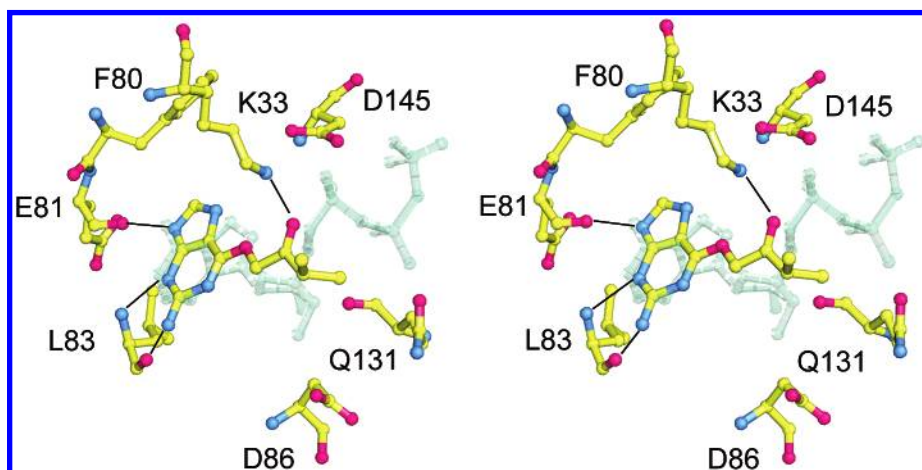


**Figure 6.** Comparative stereoview of compound **22** and ATP bound to CDK2. Only selected CDK2 residues are included for clarity. CDK2 carbon atoms and those of **22** are colored yellow. Hydrogen bonds are denoted by dashed lines. All ATP atoms are drawn in green.

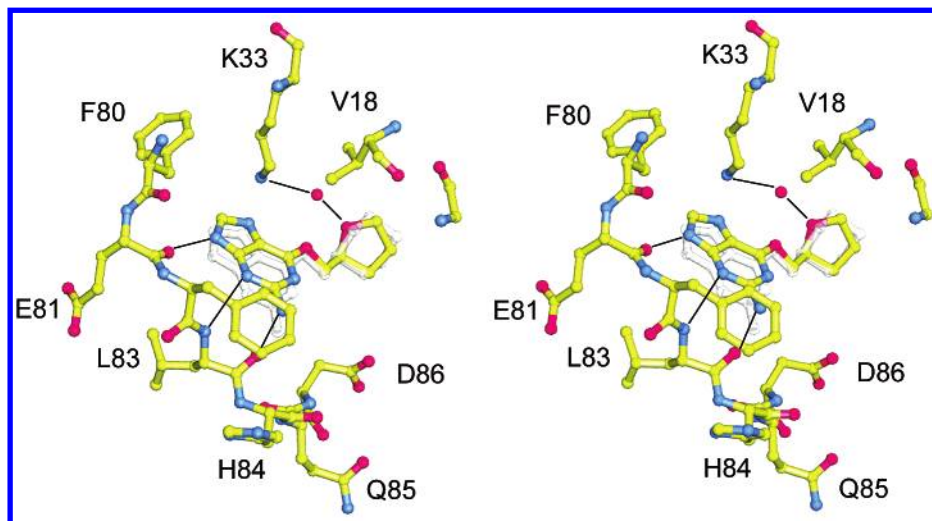


**Figure 7.** Comparative stereoview of compound **43** and NU2058 (**25**) bound to CDK2. Selected protein atoms from the CDK2/**43** complex structure are included. Hydrogen bonds are denoted by dashed lines. NU2058 is shown overlaid with all atoms of the molecule drawn in white.

an entropic penalty, which is not compensated for by these interactions in such a restricted space.

**Inhibition of Human Tumor Cell Growth by *O*<sup>6</sup>-Substituted Guanines.** The ability of three of the more potent CDK inhibitors (compounds **19**, **25**, and **27**) to

inhibit the growth of MCF7 human breast carcinoma cells was studied. As previously reported,<sup>6</sup> NU2058 (**25**) was growth-inhibited with a  $GI_{50}$  (concentration required to inhibit cell growth by 50% over a 48 h period) of  $20 \pm 9 \mu\text{M}$ . Compounds **19** and **27** had similar  $GI_{50}$

values of  $28 \pm 7$  and  $37 \pm 2$   $\mu\text{M}$ , respectively, consistent with their comparable CDK-inhibitory activity (Tables 2 and 3). Conversely, compound **44**, which produced <20% CDK1 or CDK2 inhibition at 100  $\mu\text{M}$  (Table 5), had a  $\text{GI}_{50}$  value of >100  $\mu\text{M}$  against MCF7 cells. These data are consistent with previous results showing that  $O^6$ -substituted guanine CDK inhibitors possess tumor cell growth-inhibitory activity in vitro.<sup>6</sup>

## Conclusions

The aim of the studies described in this paper was to use structure-activity studies, supported by structural analyses, to probe the ribose binding pockets of CDK1 and CDK2 in an attempt to increase the potency and individual kinase specificity of  $O^6$ -substituted guanine CDK inhibitors. SAR studies demonstrated that non-polar alkyl or cycloalkyl substituents of appropriate size (cyclohexylmethyl or similar) gave rise to maximum CDK inhibition, whereas substitution with polar groups or ring heteroatoms in cyclic systems was detrimental to inhibition. The maximum differential CDK 1 and 2 inhibition observed was 2–3-fold, which was restricted to unsubstituted  $O^6$ -cyclohexylmethyl and  $O^6$ -cyclohexenylmethyl derivatives. No compound was identified that was markedly more potent or selective than the lead inhibitor NU2058 (**25**). Consistent with the SAR data, structural analysis of selected inhibitors bound to monomeric CDK2 showed that a small hydrophobic group of defined shape at the  $O^6$ -position complements the CDK2 active site in the ribose binding pocket and leads to tight binding. The lack of any other obvious structural determinants of binding, and hence enzyme inhibition, probably reflects the highly flexible and hydrated nature of this region of the kinase active site, complicating the design of inhibitors that attempt to exploit this pocket. Furthermore, even when the ribose H-bonding interactions reported for ATP bound to monomeric CDK2 were reproduced (e.g., with Asp86 and Gln131),<sup>7</sup> as was the case for compound **56**, a reduction and not an increase in CDK inhibition was observed. Together with recent studies of ligand binding to the fully active phosphoCDK2/cyclin A complex (manuscript in preparation), which have shown a considerably larger degree of protein plasticity for this region than observed in complexes with monomeric CDK2, the data reported here imply that the ribose binding pocket will be difficult to exploit in the development of potent and selective CDK inhibitors. In contrast, substitutions on the 2-amino group of NU2058 (**25**) have resulted in inhibitors of considerably greater potency (ca. 1000-fold), and these are currently the subject of detailed biological, structural, and chemical evaluation.<sup>24,25</sup>

## Experimental Section

Melting points were obtained on a Stuart Scientific SMP3 apparatus and are uncorrected. Infrared spectra (IR) were recorded as KBr disks on a Nicolet 20 PC Fourier Transform spectrometer or neat on an Excalibur series BioRad Spectrophotometer. Ultraviolet (UV) spectra were recorded in MeOH or EtOH on a U-2001 Hitachi Spectrophotometer. Mass spectra were determined on a Kratos MS80 spectrometer in electron impact (EI) mode or fast atom bombardment (FAB) mode using a *m*-nitrobenzyl alcohol matrix. Proton (<sup>1</sup>H) and carbon (<sup>13</sup>C) nuclear magnetic resonance (NMR) spectra were recorded at 200 and 50 MHz, respectively, on a Bruker WP 200 Spectrometer employing the deuterated solvent as internal standard.

Unless indicated otherwise, spectra were recorded in [<sup>2</sup>H<sub>6</sub>]-dimethyl sulfoxide (DMSO) as solvent. NH signals appeared as broad singlets (br s) exchangeable with D<sub>2</sub>O. Chemical shift values are quoted in parts per million (ppm), and coupling constants (*J*) are quoted in Hertz (Hz). Key: t = triplet, s = singlet, q = quartet, d = doublet, dd = double doublet, m = multiplet. The thin-layer chromatography (TLC) systems employed Merck 1.05554 aluminum sheets precoated with Kieselgel 60F<sub>254</sub> (0.2 mm) as the adsorbent and were visualized with UV light at 254 and 365 nm. Column chromatography was conducted under medium pressure on silica (Kieselgel 60, 240–400 mesh). Elemental analyses were performed in house on a Carlo-Erba Instrumentazione 1106 analyzer or by Butterworth Laboratories, Middlesex, U.K., and are within  $\pm 0.4\%$  of theory unless otherwise specified. Reagents were purchased from Aldrich Chemical Co., Gillingham, U.K., or Lancaster Synthesis and used as received unless otherwise stated. Ethanol and methanol were dried using Mg/I<sub>2</sub> and stored over 4 Å molecular sieves. Diethyl ether and THF were predried over CaCl<sub>2</sub> and distilled from sodium/benzophenone. Acetonitrile was predried over potassium carbonate and distilled from CaH. Petrol refers to that fraction in the boiling range 40–60 °C. Organic solvents from separations were dried using anhydrous MgSO<sub>4</sub>.

**Standard Procedures. Standard Procedure A.** The required alkoxide was generated in situ from sodium and the appropriate alcohol using the same alcohol or THF as solvent, before addition of 2-amino-6-chloropurine, 6-chloropurine, or 2,6-dichloropurine.<sup>26,27</sup>

**Standard Procedure B.** 6-(1-Azonio-4-azabicyclo[2.2.2]oct-1-yl)purine chloride and DABCO-purine were synthesized according to a previously published procedure.<sup>15</sup> Displacement reactions were carried out as detailed by Lembicz et al. whereby the DABCO-purine was added to the desired alkoxide, which had been generated in situ from sodium hydride (2.0 equiv) and the relevant alcohol (5.5 equiv) employing DMSO (2 mL per mmol) as solvent. Purification was achieved on a silica column or by extraction into EtOAc followed by concentration in vacuo.

**Standard Procedure C.** The reaction was carried out as detailed in Arris et al.<sup>10</sup> using sodium hydride (5 equiv) and alcohol (2 equiv) to form the desired alkoxide, with THF, DMSO, or reactant alcohol as solvent. 2-Amino-6-chloropurine (1 equiv) was added as the purine reactant.

**Compounds.** Certain of the compounds have been previously described,<sup>11</sup> and physical data for the compounds prepared here are presented in Table 6. Unless specified otherwise, chiral compounds were racemic.

**2-Amino-6-prop-2-yloxympurine (7).** Compound **7** was prepared according to standard procedure A; mp 209–210 °C. <sup>1</sup>H NMR:  $\delta$  1.4 (d, 6H, CH(CH<sub>3</sub>)<sub>2</sub>), 5.6 (m, 1H, CH(CH<sub>3</sub>)<sub>2</sub>), 6.25 (s, 2H, NH<sub>2</sub>), 7.9 (s, C<sup>8</sup>H), 12.5 (s, 1H, NH). HRMS (EI): *m/z* 259.142799 [M<sup>+</sup> C<sub>11</sub>H<sub>10</sub>N<sub>6</sub>O calcd as 259.143310]. Anal. (C<sub>8</sub>H<sub>11</sub>N<sub>5</sub>O·1.0PrOH) C, H, N.

**2-Amino-6-(1'-methyl)propyloxympurine (8).** Compound **8** was prepared according to standard procedure B; mp 88–91 °C;  $\lambda_{\text{max}}$  (CH<sub>3</sub>OH)/nm 241.6, 282.0. <sup>1</sup>H NMR:  $\delta$  1.0 (t, 3H, CH<sub>2</sub>CH<sub>3</sub>), 1.4 (d, 3H, (CHCH<sub>3</sub>)), 1.8 (m, 2H, CH<sub>2</sub>CH<sub>3</sub>), 5.5 (m, 1H, CHCH<sub>3</sub>), 6.3 (s, 2H, NH<sub>2</sub>), 7.9 (s, 1H, C<sup>8</sup>H), 12.5 (s, 1H, NH). HRMS (EI): *m/z* 207.112999 [M<sup>+</sup> C<sub>9</sub>H<sub>13</sub>N<sub>5</sub>O calcd as 207.113353]. Anal. (C<sub>9</sub>H<sub>13</sub>N<sub>5</sub>O·0.7H<sub>2</sub>O) C, H, N.

**2-Amino-6-(2'-methyl)propyloxympurine (9).** Compound **9** was prepared according to standard procedure B; mp 89–92 °C. <sup>1</sup>H NMR:  $\delta$  1.1 (d, 6H, CH(CH<sub>3</sub>)<sub>2</sub>), 2.2 (m, 1H, CH<sub>2</sub>CH(CH<sub>3</sub>)<sub>2</sub>), 4.3 (d, 2H, OCH<sub>2</sub>), 6.3 (s, 2H, NH<sub>2</sub>), 7.9 (s, 1H, C<sup>8</sup>H), 12.5 (s, 1H, NH). HRMS (EI): *m/z* 207.112446 [M<sup>+</sup> C<sub>9</sub>H<sub>13</sub>N<sub>5</sub>O calcd as 207.112010].

**2-Amino-6-(2'-methyl)butyloxympurine (10).** Compound **10** was prepared according to standard procedure A; mp 175–179 °C;  $\lambda_{\text{max}}$  (CH<sub>3</sub>OH)/nm 241.0, 281.4. <sup>1</sup>H NMR:  $\delta$  1.1, 1.3, 1.6 (m, 8H, CH<sub>3</sub>CH<sub>2</sub>CHCH<sub>3</sub>), 1.9 (m, 1H, OCH<sub>2</sub>CH), 4.3 (m, 2H, OCH<sub>2</sub>), 6.3 (s, 2H, NH<sub>2</sub>), 7.9 (s, 1H, C<sup>8</sup>H), 12.5 (s, 1H, NH). HRMS (EI): *m/z* 221.127811 [M<sup>+</sup> C<sub>10</sub>H<sub>15</sub>N<sub>5</sub>O calcd as 221.127660]. Anal. (C<sub>10</sub>H<sub>15</sub>N<sub>5</sub>O·0.8MeOH) C, H, N.



**Table 6.** Physical Data for *O*<sup>6</sup>-Alkylguanines

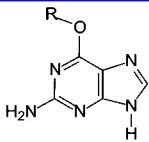
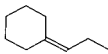
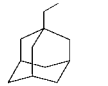
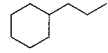
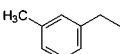
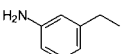
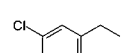
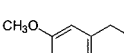
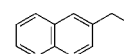
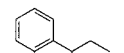
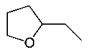
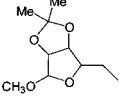
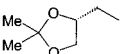
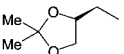
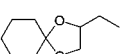
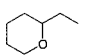
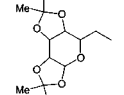
						
Compd.	R	method <sup>a</sup>	recryst. solvents <sup>b</sup>	yield (%)	formula	mp (°C)
7	<i>i</i> -Pr	B	<i>A</i>	-	C <sub>8</sub> H <sub>11</sub> N <sub>5</sub> O	209-210
8	EtCH(Me)	B	<i>B</i>	12	C <sub>9</sub> H <sub>13</sub> N <sub>5</sub> O	88-90
9	(Me) <sub>2</sub> CHCH <sub>2</sub>	B	<i>B</i>	23	C <sub>9</sub> H <sub>13</sub> N <sub>5</sub> O	89-92
10	EtCH(Me)CH <sub>2</sub>	A	<i>B</i>	71	C <sub>10</sub> H <sub>15</sub> N <sub>5</sub> O	175-179
20		B	-	11	C <sub>13</sub> H <sub>17</sub> N <sub>5</sub> O	198-200 <sup>c</sup>
29		C	-	9	C <sub>16</sub> H <sub>21</sub> N <sub>5</sub> O	230 <sup>c</sup>
30		B	-	82	C <sub>13</sub> H <sub>19</sub> N <sub>5</sub> O	209-210
32		B	<i>B</i>	49	C <sub>13</sub> H <sub>13</sub> N <sub>5</sub> O	202-203
33		B	<i>C</i>	71	C <sub>12</sub> H <sub>12</sub> N <sub>6</sub> O	152-153
34		B	<i>C</i>	63	C <sub>12</sub> H <sub>10</sub> ClN <sub>5</sub> O	220-221
35		B	<i>C</i>	72	C <sub>13</sub> H <sub>13</sub> N <sub>5</sub> O <sub>2</sub>	119
37		B	-	65	C <sub>16</sub> H <sub>13</sub> N <sub>5</sub> O	230-234
38		B	-	57	C <sub>16</sub> H <sub>13</sub> N <sub>5</sub> O	165-170
39	HOCH <sub>2</sub> CH(OH)CH <sub>2</sub>	B	<i>C</i>	87	C <sub>8</sub> H <sub>11</sub> N <sub>5</sub> O <sub>3</sub>	250-251
40	MeOCH <sub>2</sub> -CH(OMe)CH <sub>2</sub>	A	-	50	C <sub>10</sub> H <sub>13</sub> N <sub>5</sub> O <sub>3</sub>	179-180
43		B	-	27	C <sub>10</sub> H <sub>13</sub> N <sub>5</sub> O <sub>2</sub>	224-228
44		B	-	74	C <sub>14</sub> H <sub>19</sub> N <sub>5</sub> O <sub>5</sub>	220-225
46		B	-	98	C <sub>11</sub> H <sub>13</sub> N <sub>5</sub> O <sub>3</sub>	189-191
47		B	-	98	C <sub>11</sub> H <sub>13</sub> N <sub>5</sub> O <sub>3</sub>	165-167
49		B	-	92	C <sub>14</sub> H <sub>19</sub> N <sub>5</sub> O <sub>3</sub>	210-211
50		B	-	65	C <sub>11</sub> H <sub>13</sub> N <sub>5</sub> O <sub>2</sub>	255-260
51		B	-	54	C <sub>17</sub> H <sub>23</sub> N <sub>5</sub> O <sub>6</sub>	147-149

Table 6 (Continued)

Compd.	R	method <sup>a</sup>	recryst. solvents <sup>b</sup>	yield (%)	formula	mp (°C)
52		B	-	62	C <sub>14</sub> H <sub>13</sub> N <sub>5</sub> O <sub>3</sub>	184–185
53		B	-	12	C <sub>11</sub> H <sub>16</sub> N <sub>6</sub> O	221–223
54		B	D	14	C <sub>11</sub> H <sub>16</sub> N <sub>6</sub> O	250 <sup>c</sup>
55		B	-	87	C <sub>10</sub> H <sub>12</sub> N <sub>6</sub> O <sub>2</sub>	150–151
56		B	-	46	C <sub>10</sub> H <sub>12</sub> N <sub>6</sub> O <sub>2</sub>	147–148

<sup>a</sup> See the Experimental Section. <sup>b</sup> Recrystallization solvents: A, IPA; B, EtOH/petrol; C, H<sub>2</sub>O; D, EtOH/H<sub>2</sub>O. <sup>c</sup> Decomposes.

**2-Amino-6-(2'-cyclohexylidenethoxy)purine (20).** Compound **20** was prepared according to standard procedure B and decomposed at 198–200 °C. IR: 3504, 3397, 2933, 1621 cm<sup>-1</sup>. <sup>1</sup>H NMR:  $\delta$  1.6–2.2 (m, 10H, C<sub>6</sub>H<sub>10</sub>), 4.9 (d, 2H, *J* = 7.3 Hz, CH<sub>2</sub>), 5.4 (t, 1H, *J* = 7.3 Hz, =CH), 6.2 (s, 1H, NH<sub>2</sub>), 7.8 (s, 1H, C<sup>8</sup>H), 12.4 (s, 1H, NH). Anal. (C<sub>13</sub>H<sub>17</sub>N<sub>5</sub>O·0.5DMSO) C, H, N.

**2-Amino-6-adamantylmethoxypurine (29).** Compound **29** was prepared according to standard procedure C and decomposed at 230 °C;  $\lambda_{\text{max}}$  (CH<sub>3</sub>OH)/nm 282. IR: 3500, 3315, 1622 cm<sup>-1</sup>. <sup>1</sup>H NMR:  $\delta$  1.92 (m, 13H, C<sub>6</sub>H<sub>12</sub>), 2.1 (s, 3H, CH<sub>3</sub>), 4.1 (s, 2H, OCH<sub>2</sub>), 6.35 (s, 2H, NH<sub>2</sub>), 7.9 (s, 1H, C<sup>8</sup>H), 12.5 (s, 1H, NH). MS (EI): *m/z* 299 [M<sup>+</sup>], 151, 135. Anal. (C<sub>16</sub>H<sub>21</sub>N<sub>5</sub>O·0.75H<sub>2</sub>O) C, H, N.

**2-Amino-6-(2-cyclohexyl)ethoxypurine (30).** Compound **30** was prepared according to standard procedure B; mp 209–210 °C. IR: 3498, 3132, 2788, 1458 cm<sup>-1</sup>. <sup>1</sup>H NMR:  $\delta$  1.0 (m, 2H, CH<sub>2</sub>), 1.2–2.0 (m, 11H), 4.5 (t, 2H, OCH<sub>2</sub>), 6.3 (s, 2H, NH<sub>2</sub>), 7.9 (s, 1H, C<sup>8</sup>H), 12.5 (s, 1H, NH). MS (EI): *m/z* 261 [M<sup>+</sup>]. Anal. (C<sub>13</sub>H<sub>19</sub>N<sub>5</sub>O) C, H, N.

**2-Amino-6-(3'-methylbenzyl)oxypurine (32).** Compound **32** was prepared according to standard procedure B; mp 202–203 °C;  $\lambda_{\text{max}}$  (CH<sub>3</sub>OH)/nm 241.0, 296.5. IR: 3390, 3330, 2790, 1640, 1590 cm<sup>-1</sup>. <sup>1</sup>H NMR:  $\delta$  2.4 (s, 3H, CH<sub>3</sub>), 5.5 (s, 2H, OCH<sub>2</sub>), 6.4 (s, 2H, NH<sub>2</sub>), 7.4 (m, 4H, ArH), 7.9 (s, 1H, C<sup>8</sup>H). HRMS (EI): *m/z* 255.112537 [M<sup>+</sup> calcd as 255.112010]. Anal. (C<sub>13</sub>H<sub>13</sub>N<sub>5</sub>O·0.5H<sub>2</sub>O, 0.5MeOH) C, H, N.

**2-Amino-6-(3'-aminobenzyl)oxypurine (33).** Compound **33** was prepared according to standard procedure B; mp 152.5–153 °C;  $\lambda_{\text{max}}$  (CH<sub>3</sub>OH)/nm 284, 240, 219. IR: 3008.8, 2887.7, 2783.9, 1627.1, 1588.8, 1455.2, 1375.6, 1326.6, 1273.2, 1087.8 cm<sup>-1</sup>. <sup>1</sup>H NMR:  $\delta$  7.78 (1H, CH=), 7.07 (1H, t), 6.72 (1H, brs), 6.65 (2H, *H*, dd), 6.57 (1H, dd), 6.31 (1H, s, NH), 5.39 (2H, s, OCH<sub>2</sub>), 5.15 (2H, s, NH<sub>2</sub>). HRMS (EI): *m/z* 256.107079 [M<sup>+</sup> C<sub>12</sub>H<sub>12</sub>N<sub>6</sub>O calcd as 256.107259], 256, 106. Anal. (C<sub>12</sub>H<sub>12</sub>N<sub>6</sub>O) C, H, N.

**2-Amino-6-(3'-chlorobenzyl)oxypurine (34).** Compound **34** was prepared according to standard procedure B; mp 220–221 °C;  $\lambda_{\text{max}}$  (CH<sub>3</sub>OH)/nm 283, 241, 215. IR: 3411.4, 3304.0, 3172.9, 3109.2, 2957.9, 1627.9, 1584.0, 1449.4, 1400.5, 1348.0, 1276.0, 1025.8, 942.9, 785.0, 677.0, 628.8 cm<sup>-1</sup>. <sup>1</sup>H NMR:  $\delta$  7.96 (1H, CH=), 7.68 (1H, s, CH=), 7.60–7.52 (3H, 3 CH=), 6.60 (2H, s, NH<sub>2</sub>), 3.47 (2H, s, CH<sub>2</sub>O), 4.22 (1H, brs). HRMS (EI): *m/z* 275.057388 [M<sup>+</sup> C<sub>12</sub>H<sub>10</sub>ClN<sub>5</sub> calcd as 275.058044], 275, 125, 135. Anal. (C<sub>12</sub>H<sub>10</sub>ClN<sub>5</sub>O·1.0MeOH) C, H, N.

**2-Amino-6-(3'-methoxybenzyl)oxypurine (35).** Compound **35** was prepared according to standard procedure B; mp 119 °C;  $\lambda_{\text{max}}$  (CH<sub>3</sub>OH)/nm 283, 242, 215. IR: 3495.6, 3421.7, 3321.4, 3130.5, 2840.5, 1632.1, 1583.6, 1357.9, 1284.6, 1150.1, 999.7 cm<sup>-1</sup>. <sup>1</sup>H NMR:  $\delta$  7.82 (1H, CH=), 7.30 (1H, t, CH=), 7.06–7.04 (2H, 2 CH=), 6.90 (1H, dd, CH=), 6.27 (2H, s, NH<sub>2</sub>), 5.44 (2H, s, CH<sub>2</sub>O), 4.09 (1H, s, NH), 3.75 (3H, s, OCH<sub>3</sub>). HRMS (EI): *m/z* 271.106925 [M<sup>+</sup> C<sub>13</sub>H<sub>13</sub>N<sub>5</sub>O<sub>2</sub> calcd as 271.107735], 271, 121, 135, 91. Anal. (C<sub>13</sub>H<sub>13</sub>N<sub>5</sub>O<sub>2</sub>·1.0H<sub>2</sub>O) C, H, N.

**2-Amino-6-(2'-naphthyl)methoxypurine (37).** Compound **37** was prepared according to standard procedure B; mp 230–234 °C;  $\lambda_{\text{max}}$  (CH<sub>3</sub>OH)/nm 281. IR: 3335, 2562, 1642, 1585 cm<sup>-1</sup>. <sup>1</sup>H NMR:  $\delta$  5.75 (s, 2H, OCH<sub>2</sub>), 6.4 (s, 2H, NH<sub>2</sub>), 7.7 (m, 3H, C<sub>10</sub>H<sub>7</sub>), 8.05 (m, 5H, C<sup>8</sup>H and C<sub>10</sub>H<sub>7</sub>). MS (EI): *m/z* 291 [M<sup>+</sup>], 141, 95, 81. Anal. (C<sub>16</sub>H<sub>13</sub>N<sub>5</sub>O·0.01CH<sub>2</sub>Cl<sub>2</sub>) C, H, N.

**2-Amino-6-(1'-naphthyl)methoxypurine (38).** Compound **38** was prepared according to standard procedure B; mp 165–170 °C. IR: 3424, 2971, 2638, 1635, 1579 cm<sup>-1</sup>. <sup>1</sup>H NMR:  $\delta$  6.1 (s, 2H, OCH<sub>2</sub>), 6.5 (s, 2H, NH<sub>2</sub>), 7.9 (m, 8H, C<sup>8</sup>H and C<sub>10</sub>H<sub>7</sub>). MS (EI): *m/z* 291 [M<sup>+</sup>], 141, 81. Anal. (C<sub>16</sub>H<sub>13</sub>N<sub>5</sub>O·0.01CH<sub>2</sub>Cl<sub>2</sub>) C, H, N.

**2-Amino-6-(2',3'-dihydroxy)propoxyguanine (39).** **2,2-Dimethyl-1,3-dioxolan-4-ylmethoxyguanine 45** (1.79 mmol) was suspended in H<sub>2</sub>O (9.5 mL), and acetic acid was added dropwise until all of the starting material dissolved. The reaction mixture was left to stir at ambient temperature for 17 days. After this time, the solvents were removed under pressure and the product was recrystallized from water to furnish the desired product as a white solid (1.56 mmol; 87%); mp 250–251 °C. IR: 3437, 3363, 3107 cm<sup>-1</sup>. <sup>1</sup>H NMR:  $\delta$  3.6 (m, 2H, C<sup>2</sup>H<sub>2</sub>), 3.9 (m, 1H, C<sup>1</sup>H), 4.4 (m, 2H, OCH<sub>2</sub>), 4.8 (t, 1H, C<sup>2</sup>OH), 5.1 (d, 1H, C<sup>1</sup>OH), 6.3 (s, 2H, NH<sub>2</sub>), 7.9 (s, 1H, C<sup>8</sup>H). <sup>13</sup>C NMR:  $\delta$  161.0, 160.0, 155.3, 138.0, 114.0, 70.0, 67.9, 63.1. HRMS (EI): *m/z* 225.0862 [M<sup>+</sup> calcd for C<sub>8</sub>H<sub>11</sub>N<sub>5</sub>O<sub>3</sub> 225.08618], 194, 151, 134.

**2-Amino-6-(2',3'-dimethoxy)propoxypurine (40).** Compound **40** was prepared according to standard procedure A; mp 179–180 °C. IR: 3482, 3380, 3231, 2965, 2911, 2847, 2772, 2557 cm<sup>-1</sup>. <sup>1</sup>H NMR:  $\delta$  3.3 (s, 6H, 2OCH<sub>3</sub>), 4.4 (s, 2H, OCH<sub>2</sub>), 4.8 (t, 1H, *J* = 5.5 Hz, CH<sub>2</sub>CH), 6.3 (s, 2H, NH<sub>2</sub>), 7.8 (s, 1H, C<sup>8</sup>H). MS (EI): *m/z* 239 [M<sup>+</sup>], 208, 151, 134, 75.

**2-Amino-6-(2'-tetrahydrofuran-yl)methoxypurine (43).** Standard procedure C yielded the title product and starting material as a 50:50 mixture (0.26 g), which was further dissolved in anhydrous DMSO (5.0 mL), and 1,4-diazabicyclo-[2.2.2]octane (0.09 g, 0.8 mmol) was added. The reaction mixture was stirred at 25 °C for 24 h. The reactant solvents were removed under pressure, and the crude product was purified by column chromatography (10% MeOH/DCM); mp 224–228 °C;  $\lambda_{\text{max}}$  (CH<sub>3</sub>OH)/nm 283. IR: 3331, 2976, 2550, 1625 cm<sup>-1</sup>. <sup>1</sup>H NMR:  $\delta$  1.9 (m, 4H, C<sup>2</sup>H and C<sup>3</sup>H), 3.85 (m, 2H, C<sup>4</sup>H), 4.3 (m, 1H, C<sup>5</sup>H), 4.5 (d, 2H, *J* = 4.5 Hz, OCH<sub>2</sub>), 6.4 (s, 2H, NH<sub>2</sub>), 7.95 (s, 1H, C<sup>8</sup>H). <sup>13</sup>C NMR:  $\delta$  25.5 (C<sup>3</sup>), 28.0 (C<sup>2</sup>), 67.8 (C<sup>4</sup>), 67.9 (C<sup>1</sup>), 76.5 (OCH<sub>2</sub>), 113.8 (C<sup>5</sup>), 138.1 (C<sup>8</sup>), 155.5 (C<sup>6</sup>), 160.0 (C<sup>2</sup>), 160.4 (C<sup>5</sup>). MS (EI): *m/z* 235 [M<sup>+</sup>], 165, 151, 134, 78. Anal. (C<sub>10</sub>H<sub>13</sub>N<sub>5</sub>O<sub>2</sub>·0.01CH<sub>2</sub>Cl<sub>2</sub>) C, H, N.

**O<sup>6</sup>-[2-Methoxy-3,4-di-O-isopropylidene-D-ribose-5-yl]guanine (44).** Compound **44** was prepared according to standard procedure B employing methyl-2,3-O-isopropylidene- $\beta$ -D-ribofuranoside;<sup>28</sup> mp 220–225 °C;  $\lambda_{\text{max}}$  (CH<sub>3</sub>OH)/nm 283. IR: 3498 (NH), 2937 cm<sup>-1</sup>. <sup>1</sup>H NMR:  $\delta$  1.37 (3H, s, CH<sub>3</sub>), 1.49 (3H, s, CH<sub>3</sub>), 3.34 (3H, s, OCH<sub>3</sub>), 4.51 (3H, m, OCH<sub>2</sub> and C(4)H), 4.75 (1H, d, H<sub>2</sub>, *J* = 6 Hz), 4.91 (1H, d, C(3)H, *J* = 6 Hz), 5.07 (1H,

s, C(1)H), 6.41 (2H, s, NH<sub>2</sub>), 7.93 (1H, s, C(8)H), 12.5 (1H, br s, NH). MS (EI): *m/z* 337 [M<sup>+</sup>]. Anal. (C<sub>14</sub>H<sub>19</sub>N<sub>5</sub>O<sub>5</sub>·0.75 H<sub>2</sub>O) C, H, N.

**2-Amino-6-[(*R*)-2',2'-dimethyl-1',3'-dioxolane-5'-yl]-methoxypurine (46).** Compound **46** was prepared according to standard procedure B; mp 189–191 °C. <sup>1</sup>H NMR: δ 1.4 (d, 6H, 2CH<sub>3</sub>), 3.85 (m, 1H), 4.2 (m, 1H), 4.6 (m, 3H), 6.4 (s, 2H, NH<sub>2</sub>), 7.95 (s, 1H, C<sup>8</sup>H), 12.5 (s, 1H, NH). MS (EI): *m/z* 265 [M<sup>+</sup>]. Anal. (C<sub>11</sub>H<sub>15</sub>N<sub>5</sub>O<sub>3</sub>·0.5H<sub>2</sub>O) C, H, N.

**2-Amino-6-[(*S*)-2',2'-dimethyl-1',3'-dioxolane-5'-yl]-methoxypurine (47).** Compound **47** was prepared according to standard procedure B; mp 165–167 °C. IR: 3436, 2755, 1455, 1371 cm<sup>-1</sup>. <sup>1</sup>H NMR: δ 1.4 (d, 6H, 2CH<sub>3</sub>), 3.9 (m, 1H), 4.2 (m, 1H), 4.6 (m, 3H), 6.35 (s, 2H, NH<sub>2</sub>), 7.95 (s, 1H, C<sup>8</sup>H), 12.6 (s, 1H, NH). MS (EI): *m/z* 265 [M<sup>+</sup>]. Anal. (C<sub>11</sub>H<sub>15</sub>N<sub>5</sub>O<sub>3</sub>) C, H, N.

**2-Amino-6-(cyclohexylidene-2-yl)methoxypurine (49).** Compound **49** was prepared according to standard procedure B; mp 210–211 °C; λ<sub>max</sub> (CH<sub>3</sub>OH)/nm 283. IR: 3477, 3182, 2937, 1618 cm<sup>-1</sup>. <sup>1</sup>H NMR: δ 1.6 (m, 10H, C<sub>5</sub>H<sub>10</sub>), 4.0 (m, 1H, C<sup>3</sup>H), 4.5 (m, 3H, OCH<sub>2</sub> and C<sup>2</sup>H), 6.4 (s, 2H, NH<sub>2</sub>), 7.9 (s, 1H, C<sup>8</sup>H). <sup>13</sup>C NMR: δ 23.7 (C<sup>7</sup>), 23.9 (C<sup>8</sup>), 24.9 (C<sup>6</sup>), 34.9 (C<sup>9</sup>), 36.3 (C<sup>5</sup>), 65.9 (C<sup>2</sup>), 66.6 (C<sup>2</sup>), 73.5 (OCH<sub>2</sub>), 109.6 (C<sup>3</sup>), 138.7 (C<sup>8</sup>), 159.9 (C<sup>2</sup>). MS (EI): *m/z* 305 [M<sup>+</sup>], 262, 208, 151, 81. Anal. (C<sub>14</sub>H<sub>19</sub>N<sub>5</sub>O<sub>3</sub>·0.05CH<sub>2</sub>Cl<sub>2</sub>) C, H, N.

**2-Amino-6-(2'-tetrahydropyranyl)methoxypurine (NU6019-50).** This compound was prepared according to standard procedure B; mp 255–260 °C; λ<sub>max</sub> (CH<sub>3</sub>OH)/nm 283. IR: 3336, 2940, 2563, 1626, 1587 cm<sup>-1</sup>. <sup>1</sup>H NMR: δ 1.6 (m, 6H, C<sub>4</sub>H<sub>6</sub>), 3.5 (m, 1H, C<sup>5</sup>H<sub>ax</sub>), 3.7 (m, 1H, C<sup>1</sup>H<sub>ax</sub>), 4.0 (m, 1H, C<sup>5</sup>H<sub>eq</sub>), 4.4 (m, 2H, OCH<sub>2</sub>), 6.4 (s, 2H, NH<sub>2</sub>), 7.9 (s, 1H, C<sup>8</sup>H), 12.5 (s, 1H, NH). <sup>13</sup>C NMR: δ 22.9 (C<sup>3</sup>), 25.8 (C<sup>4</sup>), 27.9 (C<sup>2</sup>), 67.5 (C<sup>5</sup>), 68.7 (C<sup>4</sup>), 75.4 (OCH<sub>2</sub>), 113.8 (C<sup>5</sup>), 138.0 (C<sup>8</sup>), 155.4 (C<sup>4</sup>), 160.0 (C<sup>2</sup>), 160.4 (C<sup>6</sup>). MS (EI): *m/z* 249 [M<sup>+</sup>], 165, 151. Anal. (C<sub>11</sub>H<sub>15</sub>N<sub>5</sub>O<sub>2</sub>·0.01CH<sub>2</sub>Cl<sub>2</sub>) C, H, N.

**6-[2',3',4',5'-di-*O*-isopropylidene-*D*-galactos-6'-yl]guanine (51).** Compound **51** was prepared according to standard procedure C employing 1,2,3,4-*O*-di-isopropylidene- $\alpha$ -*D*-galactopyranose;<sup>29</sup> mp 147–149 °C. IR: 3459, 3200, 2936, 1625 cm<sup>-1</sup>. <sup>1</sup>H NMR: δ 1.4 (d, 6H, *J* = 7 Hz, 2CH<sub>3</sub>), 1.5 (s, 6H, 2CH<sub>3</sub>), 4.3 (m, 1H, C<sup>3</sup>H), 4.5 (m, 3H, OCH<sub>2</sub> and C<sup>2</sup>H), 4.6 (dd, 1H, *J* = 7 Hz, C<sup>3</sup>H), 4.7 (dd, 1H, *J* = 7 Hz, C<sup>4</sup>H), 5.6 (d, 1H, *J* = 5 Hz, C<sup>3</sup>H), 6.4 (s, 2H, NH<sub>2</sub>), 7.9 (s, 1H, C<sup>8</sup>H), 8.0 (s, 1H, NH). MS (EI): *m/z* 393 [M<sup>+</sup>]. Anal. (C<sub>17</sub>H<sub>23</sub>N<sub>5</sub>O<sub>6</sub>·0.01 M CH<sub>2</sub>Cl<sub>2</sub>) C, H, N.

**2-Amino-6-[1',4'-benzodioxan-2'-yl]methoxypurine (52).** Compound **52** was prepared according to standard procedure B; mp 184–185 °C. IR: 3439, 3157, 2886, 1629 cm<sup>-1</sup>. <sup>1</sup>H NMR: δ 4.25 (m, 1H), 4.5 (m, 1H), 4.8 (m, 3H), 6.4 (s, 2H, NH<sub>2</sub>), 7.0 (m, 4H), 7.95 (s, 1H, C<sup>8</sup>H), 12.6 (s, 1H, NH). MS (EI): *m/z* 299 [M<sup>+</sup>]. Anal. (C<sub>14</sub>H<sub>13</sub>N<sub>5</sub>O<sub>3</sub>) C, H, N.

**2-Amino-6-(piperidin-3'-ylmethyl)oxypurine (53).** Compound **53** was prepared according to standard procedure B; mp 221–223 °C; λ<sub>max</sub> (CH<sub>3</sub>OH)/nm 243.5, 284.0. IR: 3340, 3180, 1590 cm<sup>-1</sup>. HRMS (EI): *m/z* 248.138496 (M<sup>+</sup> calcd for C<sub>11</sub>H<sub>16</sub>N<sub>6</sub>O 248.138559). <sup>1</sup>H NMR: δ 1.4 (m, 1H), 1.7 (m, 1H), 1.9 (m, 2H), 2.2 (s, 1H, NH), 2.8 (m, 2H), 3.2 (m, 2H), 3.4 (d, 1H), 4.3 (d, 2H, OCH<sub>2</sub>), 7.8 (s, 1H, C<sup>8</sup>H). Anal. (C<sub>11</sub>H<sub>16</sub>N<sub>6</sub>O·1.2C<sub>2</sub>H<sub>4</sub>O<sub>2</sub>) C, H, N.

**2-Amino-6-(piperidin-3'-ylmethyl)oxypurine (54).** Compound **54** was prepared according to standard procedure B and decomposed at 250 °C; λ<sub>max</sub> (CH<sub>3</sub>OH)/nm 242.0, 283.5. IR: 3340, 3180, 1590 cm<sup>-1</sup>. HRMS (EI): *m/z* 248.139446 (M<sup>+</sup> calcd for C<sub>11</sub>H<sub>16</sub>N<sub>6</sub>O 248.138559). <sup>1</sup>H NMR: δ 1.6 (m, 2H, CH<sub>2</sub>CH<sub>2</sub>-NH), 2.1 (d, 2H, CH<sub>2</sub>CH<sub>2</sub>NH), 2.2 (s, 1H, NH), 3.0 (d.t, 2H, CH<sub>2</sub>CH<sub>2</sub>NH), 3.3 (m, 2H, CH<sub>2</sub>CH<sub>2</sub>NH), 3.6 (d, 1H, CH<sub>2</sub>CH), 4.4 (d, 2H, OCH<sub>2</sub>), 7.9 (s, 1H, C<sup>8</sup>H). Anal. (C<sub>11</sub>H<sub>16</sub>N<sub>6</sub>O·1.3H<sub>2</sub>O, 1.3C<sub>2</sub>H<sub>4</sub>O<sub>2</sub>) C, H, N.

**2-Amino-6-[(*S*)-pyrrolidinon-5'-yl]methoxypurine (55).** Compound **55** was prepared according to standard procedure B; mp 150–151 °C. IR: 3348, 3113, 2796, 1450 cm<sup>-1</sup>. <sup>1</sup>H NMR: δ 2.0 (m, 1H), 2.3 (m, 3H), 4.0 (m, 1H), 4.4 (d, 2H, OCH<sub>2</sub>), 6.4 (s, 2H, NH<sub>2</sub>), 7.95 (s, 2H, C<sup>8</sup>H, NH). MS (EI): *m/z* 248 [M<sup>+</sup>]. Anal. (C<sub>10</sub>H<sub>12</sub>N<sub>6</sub>O<sub>2</sub>·1.5H<sub>2</sub>O) C, H, N.

**2-Amino-6-[(*R*)-pyrrolidinon-5'-yl]methoxypurine (56).** Compound **56** was prepared according to standard procedure B; mp 146–148 °C. <sup>1</sup>H NMR: δ 2.0 (m, 1H), 2.35 (m, 3H), 4.05 (m, 1H), 4.45 (d, 2H, OCH<sub>2</sub>), 6.4 (s, 2H, NH<sub>2</sub>), 7.9 (s, 2H, C<sup>8</sup>H, NH). MS (EI): *m/z* 248 [M<sup>+</sup>]. Anal. (C<sub>10</sub>H<sub>12</sub>N<sub>6</sub>O<sub>2</sub>·1.0H<sub>2</sub>O) C, H, N.

**2-Amino-6-(3'-pyridyl)methoxypurine (58).** Compound **58** was prepared as reported previously by Kohda et al and McElhinney et al.<sup>14,30</sup>

**Expression, Purification, and Crystallization of Human CDK2.** Human CDK2 was expressed in Sf9 insect cells using a recombinant baculovirus encoding CDK2 and purified following slight modifications to a published method.<sup>6</sup> Monomeric unphosphorylated CDK2 crystals were grown as previously described.<sup>31</sup>

**X-ray Crystallography Data Collection and Processing.** Crystals of CDK2 were soaked for approximately 48 h in 5 mM inhibitor in crystallization well solution (50 mM ammonium acetate, 10% PEG 3350, 15 mM NaCl, 100 mM HEPES, pH 7.4) plus 5% DMSO. Immediately prior to data collection, the crystals were transferred briefly to cryoprotectant (mother liquor containing 20% glycerol) before flash-freezing in an Oxford Cryostream at 100 K. X-ray diffraction data were collected at the ESRF, the Synchrotron Radiation Source, Daresbury, and the Elettra Light source. Images were integrated using Denzo<sup>32</sup> or Mosflm<sup>33</sup> and subsequently scaled and merged using Scalepack<sup>32</sup> or Scala.<sup>34</sup> Data collection and processing statistics are available in the Supporting Information.

**Structure Solution and Refinement.** The starting model for the structure solution and refinement of the CDK2–**22** complex was a model of CDK2 from a complex with another inhibitor of the purine-based series (unpublished data). Refinement of the structure was begun by carrying out rigid body refinement using REFMAC,<sup>35</sup> using both sequentially higher resolution data and an increasing number of rigid body fragments. Following rigid body refinement, the (*F*<sub>o</sub> – *F*<sub>c</sub>)<sub>calc</sub> maps included readily interpretable electron density for the bound inhibitor. The ligand was built assuming ideal geometry in SYBYL and subsequently fitted into the difference electron density using "O".<sup>36</sup> The resulting complex was then subjected to alternating cycles of manual model rebuilding and maximum likelihood refinement using REFMAC.<sup>35</sup> Individual anisotropic temperature factor refinement was implemented throughout, and hydrogen atoms were added and included in the refinement although they were omitted from the final model. Toward the end of refinement, water molecules were added using ARP.<sup>37</sup> In view of the high-resolution data available for the refinement of the CDK2–**22** complex, the resulting structure was subsequently used as a model for refinement of the other three data sets using the same protocol as described above. Electron density for residues forming the activation segment was of variable quality, and residues were omitted from the final models where their positions could not be modeled with confidence. Refinement statistics are in the Supporting Information. The four structures solved in this study (of CDK2 in complex with the compounds **27**, **43**, **22**, and **56**) will be deposited with the Protein Data Bank and assigned the codes 1h0w, 1h0u, 1g28, and 1h0v, respectively. The structure of NU2058 (**25**) solved previously has been assigned the PDB code 1e1v.<sup>6</sup>

**Enzyme Inhibition Studies.** Inhibition of starfish oocyte (*Marthasterias glacialis*) CDK1/cyclin B1 and human CDK2/cyclin A was assayed as previously described.<sup>6</sup>

**Cell Growth Inhibition Studies.** The inhibition of tumor cell growth was determined using MCF-7 human breast carcinoma cells. Cells were plated at a density of 1 × 10<sup>3</sup>/well in 96 well plates containing RPMI medium (supplemented with 10% (v/v) fetal calf serum), allowed to grow for 72 h, and then treated with a range of inhibitor concentrations for 48 h (final DMSO concentration 1% (v/v)). Cell growth, relative to growth of control cells treated with 1% (v/v) DMSO alone, was measured by sulforhodamine B staining of trichloroacetic acid-precipitated cell protein as described.<sup>38</sup> The GI<sub>50</sub> concentration



for each compound was the concentration required to reduce cell growth by 50%.

**Acknowledgment.** We thank David Morgan for his generous gift of the AcCDK2 baculovirus and Tim Hunt for a human cyclin A construct. The staff at station 9.5, Daresbury, beamline BM14, ESRF, and X-RAY DIFFRACTION, Elettra, provided excellent facilities and advice during data collection. At the LMB, we thank I. Taylor, E. F. Garman, A. M. Lawrie, R. Bryan, Y. Huang, K. Measures, and S. Lee. This research was supported by grants from Cancer Research U.K., The Royal Society U.K., Medical Research Council U.K., BBSRC, and AstraZeneca PLC U.K.

**Supporting Information Available:** Data collection and refinement statistics for the four CDK2-inhibitor complexes. This material is available free of charge via the Internet at <http://pubs.acs.org>.

## References

- Senderowicz, A. M.; Sausville, E. A. Preclinical and clinical development of cyclin-dependent kinase modulators. *J. Natl. Cancer Inst.* **2000**, *92*, 376–387.
- Meijer, L.; Leclerc, S.; Leost, M. Properties and potential applications of chemical inhibitors of cyclin-dependent kinases. *Pharmacol. Ther.* **1999**, *82*, 279–284.
- Garrett, M. D.; Fattaey, A. CDK inhibition and cancer therapy. *Curr. Opin. Genet. Dev.* **1999**, *9*, 104–111.
- Gray, N.; Detivaud, L.; Doerig, D.; Meijer, L. ATP-site inhibitors of cyclin-dependent kinases. *Curr. Med. Chem.* **1999**, *6*, 859–875.
- Sielecki, T. M.; Boylan, J. F.; Benfield, P. A.; Trainor, G. L. Cyclin-dependent kinase inhibitors: Useful targets in cell cycle regulation. *J. Med. Chem.* **2000**, *43*, 1–18.
- Arris, C. E.; Boyle, F. T.; Calvert, A. H.; Curtin, N. J.; Endicott, J. A.; Garman, E. F.; Gibson, A. E.; Golding, B. T.; Grant, S.; Griffin, R. J.; Jewsbury, P.; Johnson, L. N.; Lawrie, A. M.; Newell, D. R.; Noble, M. E. M.; Sausville, E. A.; Schultz, R.; Yu, W. Identification of novel purine and pyrimidine cyclin-dependent kinase inhibitors with distinct molecular interactions and tumour cell growth inhibition profiles. *J. Med. Chem.* **2000**, *43*, 2797–2804.
- Schulze-Gahmen, U.; Brandsen, J.; Jones, H. D.; Morgan, D. O.; Meijer, L.; Vesely, J.; Kim, S.-H. Multiple modes of ligand recognition: Crystal structure of cyclin-dependent protein kinase 2 in complex with ATP and two inhibitors, olomoucine and isopentenyladenine. *Proteins* **1995**, *22*, 378–391.
- de Azevedo, W. F., Jr.; Leclerc, S.; Meijer, L.; Havlicek, L.; Strnad, M.; Kim, S.-H. Inhibition of cyclin-dependent kinases by purine analogues. Crystal structure of human cdk2 complexed with roscovitine. *Eur. J. Biochem.* **1997**, *243*, 518–526.
- Gray, N. S.; Wodicka, L.; Thunnissen, A.-M. W. H.; Norman, T. C.; Kwon, S.; Espinoza, F. H.; Morgan, D. O.; Barnes, G.; Leclerc, S.; Meijer, L.; Kim, S.-H.; Lockhart, D. J.; Schultz, P. G. Exploiting chemical libraries, structure, and genomics in the search for kinase inhibitors. *Science* **1998**, *281*, 533–538.
- Arris, C. E.; Bleasdale, C.; Calvert, A. H.; Curtin, N. J.; Dalby, C.; Golding, B. T.; Griffin, R. J.; Lunn, J. M.; Major, G. N.; Newell, D. R. Probing the active site and mechanism of action of *O*<sup>6</sup>-alkylguanine-DNA alkyltransferase with substrate analogues. *Anticancer Drug Des.* **1994**, *9*, 401–408.
- Griffin, R. J.; Arris, C. E.; Bleasdale, C.; Boyle, F. T.; Calvert, A. H.; Curtin, N. J.; Dalby, C.; Kanugula, S.; Lembicz, N. K.; Newell, D. R.; Pegg, A. E.; Golding, B. T. Resistance-Modifying Agents. 8. Inhibition of *O*<sup>6</sup>-alkylguanine-DNA alkyltransferase by *O*<sup>6</sup>-alkenyl-, *O*<sup>6</sup>-cycloalkenyl-, and *O*<sup>6</sup>-(2-oxoalkyl)guanines and potentiation of Temozolomide cytotoxicity in vitro by *O*<sup>6</sup>-(1-cyclopentenylmethyl)guanine. *J. Med. Chem.* **2000**, *43*, 4071–4083.
- Chae, M.-Y.; McDougall, M. G.; Dolan, M. E.; Swenn, K.; Pegg, A. E.; Moschel, R. C. Substituted *O*<sup>6</sup>-benzylguanines derivatives and their inactivation of human *O*<sup>6</sup>-alkylguanine-DNA alkyltransferase. *J. Med. Chem.* **1994**, *37*, 342–347.
- McCoss, M.; Chen, A.; Tolman, R. L. Synthesis of the chiral acyclonucleoside antiheteric agent (S)-9-(2,3-dihydroxy-1-propoxymethyl)guanine. *Tetrahedron Lett.* **1985**, *26*, 1815–1818.
- McElhinney, R. S.; Donnelly, D. J.; McCormick, J. E.; Kelly, J.; Watson, A. J.; Rafferty, J. A.; Elder, R. H.; Middleton, M. R.; Willington, M. A.; McMurry, T. B. H.; Margison, G. P. Inactivation of *O*<sup>6</sup>-alkylguanine-DNA alkyltransferase. 1. Novel *O*<sup>6</sup>-(hetaryl)methylguanines having basic rings in the side chain. *J. Med. Chem.* **1998**, *41*, 5265–5271.
- Lembicz, N. K.; Grant, S.; Clegg, W.; Griffin, R. J.; Heath, S. L.; Golding, B. T. Facilitation of displacements at the 6-position of purines by the use of 1,4-diazabicyclo[2,2,2]octane as leaving group. *J. Chem. Soc., Perkin Trans. 1* **1997**, 185–186.
- Vesely, J.; Havlicek, L.; Strnad, M.; Blow, J. J.; Donella-Deana, A.; Pinna, L.; Letham, D. S.; Kato, J.-Y.; Detivaud, L.; Leclerc, S.; Meijer, L. Inhibition of cyclin-dependent kinases by purine analogues. *Eur. J. Biochem.* **1994**, *224*, 771–786.
- Schow, S. R.; Mackman, R. L.; Blum, C. L.; Brooks, E.; Horsma, A. G.; Joly, A.; Kerwar, S. S.; Lee, G.; Schiffman, D.; Nelson, M. G.; Wang, X.; Wick, M. M.; Zhang, X.; Lum, R. T. Synthesis and activity of 2,6,9-trisubstituted purines. *Bioorg. Med. Chem. Lett.* **1997**, *7*, 2697–2702.
- Legraverend, M.; Ludwig, O.; Bisagni, E.; Leclerc, S.; Meijer, L. Synthesis of C2 alkynylated purines, a new family of potent inhibitors of cyclin-dependent kinases. *Bioorg. Med. Chem. Lett.* **1998**, *8*, 793–798.
- Imbach, P.; Capraro, H.-G.; Furet, P.; Mett, H.; Meyer, T.; Zimmermann, J. 2,6,9-Trisubstituted purines: Optimization towards highly potent and selective CDK1 inhibitors. *Bioorg. Med. Chem. Lett.* **1999**, *9*, 91–96.
- Chang, Y.-T.; Gray, N. S.; Rosania, G. R.; Sutherland, D. P.; Kwon, S.; Norman, T. C.; Sarohia, R.; Leost, M.; Meijer, L.; Schultz, P. G. Synthesis and application of functionally diverse 2,6,9-trisubstituted purine libraries as CDK inhibitors. *Chem. Biol.* **1999**, *6*, 361–375.
- Legraverend, M.; Tunnah, P.; Noble, M.; Ducrot, M.; Ludwig, O.; Grierson, D. S.; Leost, M.; Meijer, L.; Endicott, J. Cyclin-dependent kinase inhibition by new C-2 alkynylated purine derivatives and molecular structure of a CDK2-inhibitor complex. *J. Med. Chem.* **2000**, *43*, 1282–1292.
- De Bondt, H. L.; Rosenblatt, J.; Jancarik, J.; Jones, H. D.; Morgan, D. O.; Kim, S.-H. Crystal structure of cyclin-dependent kinase 2. *Nature* **1993**, *363*, 595–602.
- Russo, A.; Jeffrey, P. D.; Pavletich, N. P. Structural basis of cyclin-dependent kinase activation by phosphorylation. *Nat. Struct. Biol.* **1996**, *3*, 696–700.
- Griffin, R. J.; Arris, C. E.; Bentley, J.; Boyle, F. T.; Calvert, A. H.; Curtin, N. J.; Davies, T. G.; Jewsbury, P.; Endicott, J. A.; Golding, B. T.; Hardcastle, I. R.; Johnson, L. N.; Mesguiche, V.; Newell, D. R.; Noble, M. E. M.; Parsons, R. J.; Whitfield, H. J. Structure-based design of potent inhibitors of CDK1 and CDK2. *Proc. Am. Assoc. Cancer Res.* **2001**, *42*, 456.
- Bentley, J.; Arris, C. E.; Boyle, F. T.; Byth, K.; Calvert, A. H.; Curtin, N. J.; Davies, T. G.; Jewsbury, P.; Endicott, J. A.; Golding, B. T.; Griffin, R. J.; Hardcastle, I. R.; Johnson, L. N.; Mesguiche, V.; Newell, D. R.; Noble, M. E. M.; Parsons, R. J.; Whitfield, H. J. Cellular pharmacology of a novel potent CDK1 and CDK2 inhibitor. *Proc. Am. Assoc. Cancer Res.* **2001**, *42*, 457.
- Bowles, W. A.; Schneider, F. H.; Lewis, L. R.; Robins, R. K. Synthesis and antitumor activity of 9-(tetrahydro-2-furyl)purine analogues of biologically important deoxynucleosides. *J. Med. Chem.* **1963**, *6*, 471–480.
- Frihart, C. R.; Leonard, N. J. Allylic rearrangement from O-6 to C-8 in the guanine series. *J. Am. Chem. Soc.* **1973**, *95*, 7174–7175.
- Lewbart, M. L.; Schneider, J. J. Preparation and properties of steroidal 17,20- and 20,21-acetonides epimeric at C-20. I. Derivatives of 5B-pregnan-3 $\alpha$ -ol. *J. Org. Chem.* **1969**, *34*, 3505–3512.
- Buchanan, J. G.; Saunders, R. M. Methyl-2,3-anhydro- $\alpha$ -D-mannoside and 3,4-anhydro- $\alpha$ -D-altroside and their derivatives. Part III. *J. Chem. Soc.* **1964**, 1796–1803.
- Kohda, K.; Terashima, I.; Koyama, K.-I.; Watanabe, K.; Mineura, K. Potentiation of the cytotoxicity of chloroethylnitrosourea by *O*-6-arylmethylguanines. *Biol. Pharm. Bull.* **1995**, *18*, 424–430.
- Lawrie, A. M.; Noble, M. E. M.; Tunnah, P.; Brown, N. R.; Johnson, L. N.; Endicott, J. A. Protein kinase inhibition by staurosporine: Details of the molecular interaction determined by the X-ray crystallographic analysis of a CDK2-staurosporine complex. *Nat. Struct. Biol.* **1997**, *4*, 796–802.
- Otwiñowski, Z. In *Oscillation Data Reduction Program*; Sawyer, L.; Isaacs, N.; Bailey, S., Eds; DL/SC1/R34; SERC Laboratory: Daresbury, Warrington, U.K., 1993; pp 56–62.
- Collaborative Computational Project, Number 4. The CCP4 suite: programs for protein crystallography. *Acta Crystallogr.* **1994**, *D50*, 760–763.
- Evans, P. R. *Data Reduction*. Proceedings of CCP4 Study Weekend on Data Collection and Processing, 1993; pp 114–122.
- Murshudov, G. N.; Vagin, A. A.; Dodson, E. J. Refinement of macromolecular structures by the maximum-likelihood method. *Acta Crystallogr.* **1997**, *D53*, 240–255.
- Jones, T. A.; Zou, J. Y.; Cowan, S. W.; Kjeldgaard, M. Improved method for building models in electron density maps and the location of errors in these models. *Acta Crystallogr.* **1991**, *A47*, 110–119.
- Lamzin, V. S.; Wilson, K. S. Automated refinement of protein models. *Acta Crystallogr.* **1993**, *D49*, 129–147.

- (38) Skehan, P.; Storeng, R.; Scudiero, D.; Monks, A.; McMahon, J.; Vistica, D.; Warren, J. T.; Bokesch, H.; Kenney, S.; Boyd, M. R. New colorimetric cytotoxicity assay for anticancer-drug screening. *J. Natl. Cancer Inst.* **1990**, *82*, 1107–1112.

- (39) Goodford, P. J. A computational procedure for determining energetically favourable binding sites on biologically important macromolecules. *J. Med. Chem.* **1985**, *28*, 849–857.  
JM020056Z